IEICE TRANSACTIONS

on Information and Systems

VOL. E98-D NO. 5
MAY 2015

A PUBLICATION OF THE INFORMATION AND SYSTEMS SOCIETY
The Institute of Electronics, Information and Communication Engineers
Kikai-Shinko-Kaikan Bldg., 5-8, Shibakoen 3 chome, Minato-ku, TOKYO, 105-0011 JAPAN

PAPER

Noise Tolerant Heart Rate Extraction Algorithm Using Short-Term Autocorrelation for Wearable Healthcare Systems

Shintaro IZUMI[†a)], *Member*, Masanao NAKANO[†], Ken YAMASHITA[†], Yozaburo NAKAI[†], *Nonmembers*, Hiroshi KAWAGUCHI[†], *and* Masahiko YOSHIMOTO[†], *Members*

SUMMARY This report describes a robust method of instantaneous heart rate (IHR) extraction from noisy electrocardiogram (ECG) signals. Generally, R-waves are extracted from ECG using a threshold to calculate the IHR from the interval of R-waves. However, noise increases the incidence of misdetection and false detection in wearable healthcare systems because the power consumption and electrode distance are limited to reduce the size and weight. To prevent incorrect detection, we propose a short-time autocorrelation (STAC) technique. The proposed method extracts the IHR by determining the search window shift length which maximizes the correlation coefficient between the template window and the search window. It uses the similarity of the QRS complex waveform beat-by-beat. Therefore, it has no threshold calculation process. Furthermore, it is robust against noisy environments. The proposed method was evaluated using MIT-BIH arrhythmia and noise stress test databases. Simulation results show that the proposed method achieves a state-of-the-art success rate of IHR extraction in a noise stress test using a muscle artifact and a motion artifact.

key words: *autocorrelation, biomedical signal processing, electrocardiography, heart rate extraction, noise tolerance*

1. Introduction

Mobile and wearable healthcare devices are expected to play an increasingly prominent role in health provision due to the advent of aging societies around the world [1]. In particular, biosignal measurements during daily life at home are important to prevent lifestyle diseases, which are expected to raise the number of patients and elderly people requiring nursing care.

This report describes a noise-tolerant instantaneous heart rate (IHR) extraction algorithm from noisy ECG signals. The IHR is useful for heart disease detection, heart rate variation analysis [2], and exercise intensity estimation [3].

Key factors affecting wearable system usability are miniaturization and weight reduction. A wearable and wireless ECG telemetry system [4], [5] and single-chip ECG monitoring system LSIs [6]–[8] have been developed. However, the wearable system is sensitive to noise because of strict limitations on power consumption and electrode distance (see Fig. 1). The signal-to-noise ratio (SNR) of ECG signals can be degraded, especially if a subject is not at rest.

In general, sophisticated analog front-end circuits are necessary to prevent SNR degradation. The analog front-ends of ECG monitoring systems mainly comprise amplifiers, analog filters, and an analog-to-digital converter (ADC). Unfortunately, analog circuits have a large circuit area and high power consumption. Battery mass and power consumption must be reduced because the battery mass dominates wearable systems. The amplifier presents a tradeoff between power consumption and performance (e.g., gain, phase characteristic, common mode rejection ratio). Moreover, the analog filter in an ECG monitor has a large RC time constant because the ECG signal frequency range is low ($f < 1$ kHz). For those reasons, it is difficult to use high-performance amplifiers and analog filters that have a high quality factor.

Ultra-low-power ADCs, which have sub-microwatt power consumption and a limited sample rate, have been developed for biomedical applications [9], [10]. Furthermore, according to Moore's law, the power of digital components increases with the progress of process technology. In contrast, the power consumption of analog circuits will not decrease similarly. Therefore, as illustrated in Fig. 2, our approach using digital signal processing aims to reduce the performance requirements of analog components and to minimize the system's overall power consumption.

A preliminary version of this work has been reported in the literature [11]. This paper presents an extended version of the algorithm and additional details of performance evaluation results. Section 2 of this report describes conventional

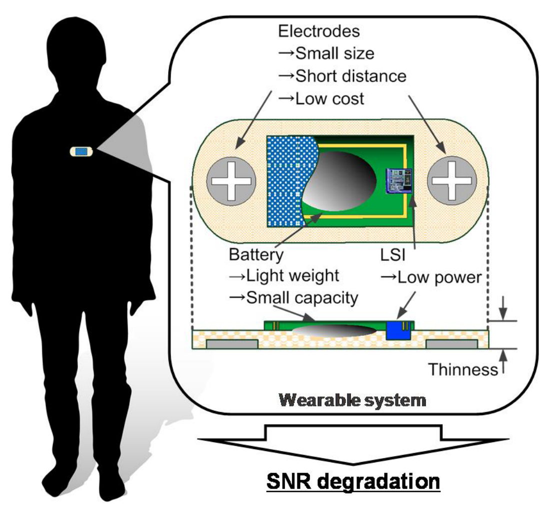

Fig. 1 Constraints of a wearable healthcare system.

Manuscript received May 17, 2014.
Manuscript revised November 16, 2014.
Manuscript publicized January 26, 2015.

[†]The authors are with the Graduate School of System Informatics, Kobe University, Kobe-shi, 657–8501 Japan.
a) E-mail: shin@cs28.cs.kobe-u.ac.jp

DOI: 10.1587/transinf.2014EDP7161

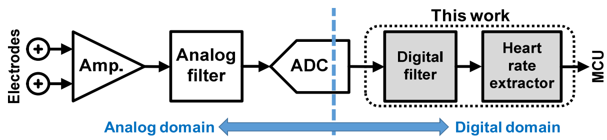

Fig. 2 Block diagram of ECG sensing circuits and target of this work.

heart rate extraction techniques. An improved heart rate extraction scheme is proposed in Sect. 3. Section 4 presents some simulation results including noise stress tests. Finally, conclusions are presented in Sect. 5.

2. Heart Rate Extraction Techniques

Recently, various algorithms have been proposed to improve heart rate extraction accuracy and reliability.

Extracting R-waves using threshold determination is a widely used approach for IHR extraction from ECG. The Pan–Tompkins (PT) algorithm [12], which is commonly used for beat detection, uses band-pass filtering, differentiation, squaring, and moving window integration. Periodically, the threshold is adjusted automatically using QRS morphology and the heart rate.

The SQRS [13] and WQRS [14] algorithms, which have been published in PhysioNet, can respectively detect QRS based on ECG slope and length transform. The SQRS uses band pass filtering for noise reduction, which uses only the integer coefficient. The WQRS also uses a low-pass filter to remove baseline wander.

The Discrete Wavelet Transform (DWT) [7], [15], [16] uses a wavelet transform with quadratic spline wavelet (QSW). The threshold is calculated using the root mean square value of the wavelet transform. This algorithm has been used in robust ECG monitoring LSIs [7], [17], [18]. The QSW requires few calculations and low hardware costs because it can be implemented using only adders and shift operators.

The Quad Level Vector (QLV) algorithm [19] is used in dedicated hardware for ECG monitoring LSI [6], [20]. The QLV is generated using DWT and the adaptive threshold. Then, the threshold is ascertained from the maximum mean deviation (MD) of prior heartbeats.

The Continuous Wavelet Transform (CWT) algorithm [21]–[23] uses a Mexican hat wavelet in the frequency interval of 15–18 Hz. The R-peak can be extracted using the adaptive threshold, which is calculated using the modulus maxima of the CWT. This algorithm was also implemented in an earlier study [6].

Figure 3 presents the heart beat detection accuracy of conventional threshold based algorithms from the 1980s [12], [15], [16], [22], [24]–[46]. As depicted in Fig. 3, no significant difference was found in the accuracy. However, these results are evaluated using only clean ECG (MIT-BIT open ECG database record #100 [47]). As depicted in Fig. 4, noise from various sources increases misdetection and false detection in the wearable healthcare system. Figure 5 (a) presents frequency characteristics of the PT, SQRS, and DWT with a 128 Hz sampling rate. Figure 5 (b) depicts the ECG and well-known noise waveforms. A baseline wander and a hum noise can be removed easily using digital filters. However, unfortunately, the frequency ranges of the muscle artifact and electrode motion artifacts are similar to those of the desired ECG signals.

Therefore, this work was undertaken for noise tolerance improvement. Threshold-based algorithms are classifiable using preprocessing and QRS detection, as presented in Table 1. Our proposed method, as described in Sect. 3,

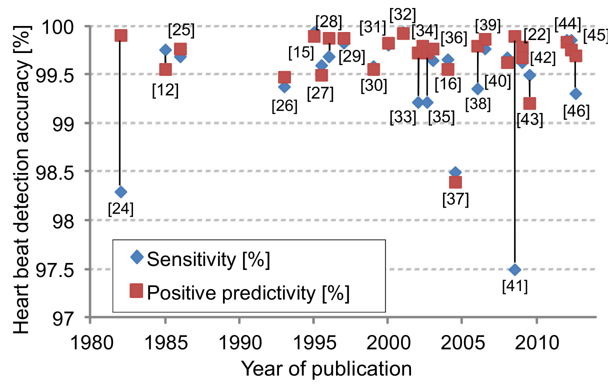

Fig. 3 Accuracy comparison of recent heart beat detection methods with MIT-BIH record #100.

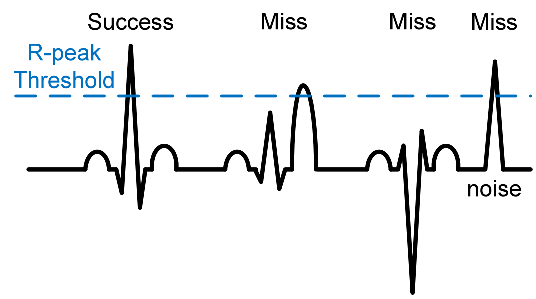

Fig. 4 Noise problem with threshold based R-peak detection.

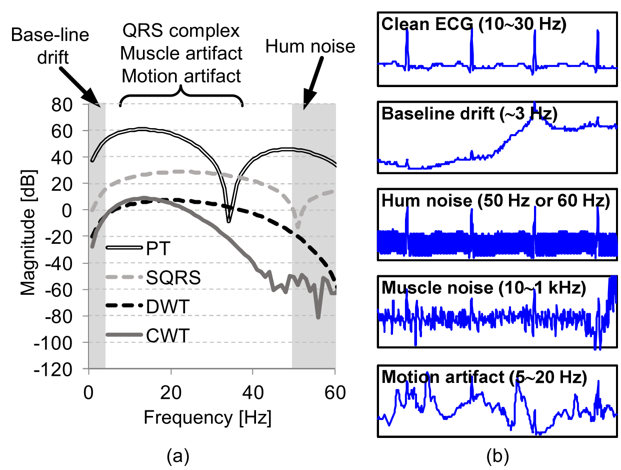

Fig. 5 (a) Frequency characteristics of filters with 128 Hz sampling rate. (b) Waveform of ECG signals with noise.

Table 1 Preprocessing and QRS detection in conventional methods.

	Preprocessing (filter technique)	QRS detection (threshold)
[12]	Bandpass filter, derivative, squaring, and moving window integrator	Signal peak and noise peak
[13]	Bandpass filter	Slope criterion
[14]	Lowpass filter and curve length transform	QRS amplitude
[16]	DWT	Root Mean Square (RMS)
[19]	Discrete wavelet transform (DWT)	Mean deviation (MD)
[22]	Continuaous wavelet transform (CWT)	Modulus maxima

can replace the threshold-based method. In other words, the proposed method can be combined with any other preprocessing filter technique shown in Table 1.

3. Short-Term Autocorrelation

In this work, we propose a short-term autocorrelation (STAC) technique for IHR extraction. Autocorrelation [48], [49] and template matching [50] use the similarity of QRS complex waveforms and have no threshold calculation process. Autocorrelation has been used in non-invasive monitoring systems. However, the method necessitates numerous computations because it calculates the average heart rate over a long duration (30 s). In this work, we extend it for IHR extraction by minimizing the window length because conventional works can only extract the average heart rate from data of a long duration. To achieve accurate heart rate variability analysis, the IHR of every second is required.

Figure 6 portrays IHR extraction using STAC. As depicted in Fig. 6 and (1–7), the recent interval of R-waves at time t_n (RR[n]) is obtained as a window shift length (T_{shift}) that maximizes the correlation coefficient between the template window and the search window (CC[n]). The IHR at t_n (IHR[n]) is calculable using RR[n], as shown in (6).

$$RR[\mathrm{n}] = \underset{RR_{\min}\le T_{\text{shift}}\le RR_{\max}}{\arg_{T_{\text{shift}}} \max} \{CC[\mathrm{n}]\} \tag{1}$$

$$CC[\mathrm{n}] = W_c(T_{\text{shift}}) \cdot \sum_{i=0}^{L_w[\mathrm{n}]} W_w(i) \cdot d[t_n - i] \cdot d[t_n - i - T_{\text{shift}}] \tag{2}$$

$$W_c(T_{\text{shift}}) = \max\left\{1 - \frac{1}{4} \cdot \left|\frac{T_{shift} - RR_{min}}{RR_{min}}\right|, \frac{1}{4}\right\} \tag{3}$$

$$W_w(i) = \max\left[1 - \frac{1}{8} \cdot \left|\frac{t}{RR_{min}}\right|, \frac{1}{8}\right] \tag{4}$$

$$L_w[\mathrm{n}] = \begin{cases} RR[\mathrm{n}-1] \times (1.2)^3 & (RR_{\min} \le RR[\mathrm{n}-1] < 0.316) \\ RR[\mathrm{n}-1] \times (1.2)^2 & (0.316 \le RR[\mathrm{n}-1] < 0.695) \\ RR[\mathrm{n}-1] \times (1.2)^1 & (0.695 \le RR[\mathrm{n}-1] \le RR_{\max}) \end{cases} \tag{5}$$

$$IHR[\mathrm{n}] = \frac{60}{RR[\mathrm{n}]} \tag{6}$$

$$t_n = t_{n-1} + 1 \tag{7}$$

In the equations presented above, W_c and W_w denote weight coefficients. As depicted in Fig. 7, W_c contributes to the choice of the recent peak of the correlation coefficient if two or more R-peaks exist in the shift range of T_{shift}; W_w contributes to the choice of the accurate peak of the correlation coefficient if two or more R-peaks exist in the template of search window because the waveform of the correlation coefficient has a bimodal peak in such a case (see Fig. 8).

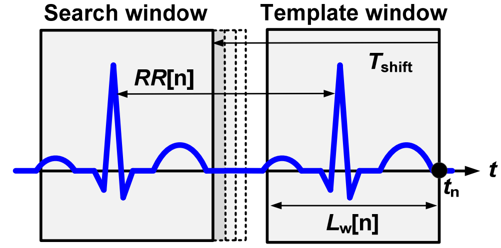

Fig. 6 IHR extraction using short-term autocorrelation (STAC).

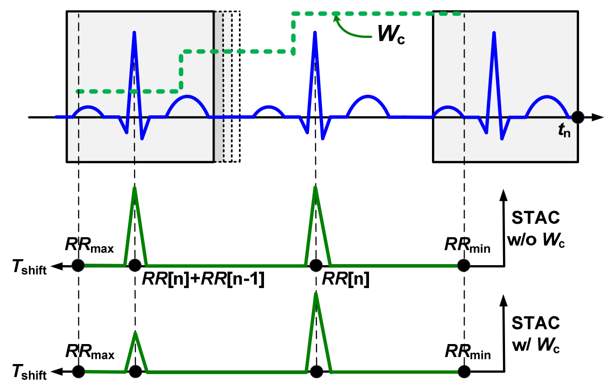

Fig. 7 Weight coefficient W_c to suppress old R-peak misdetection.

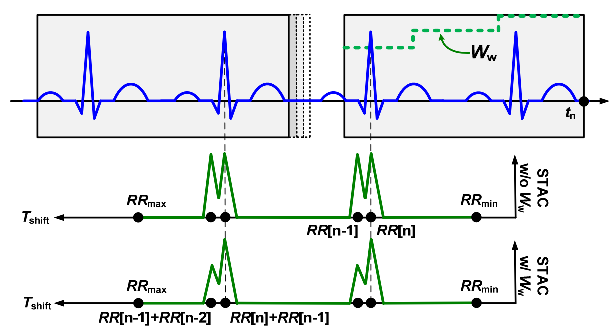

Fig. 8 Weight coefficient W_w to improve R-peak detection accuracy.

The shift range of T_{shift} is decided by maximum and minimum values of RR[n] ($RR_{\max}$ and $RR_{\min}$). In this work, $RR_{\max}$ and $RR_{\min}$ are set respectively as 0.25 s and 1.5 s because the heart rate of a healthy person is 40 bpm–240 bpm in general.

The L_w in (1) and (3) denotes the window length, which is updated according to the estimated value of RR[n] from RR[n − 1], as shown in (5). The initial value of L_w is set to 1.5 s in this work. L_w should be set to include one or more beats in the template and search windows. If RR[n − 1] is smaller than 0.316 s, then three R-waves exist between

$t_n - 1$ and t_n at maximum. Then L_w is set to $RR[n-1] \times (1.2)^3$ according to the maximum rate of the beat-to-beat variation, which is generally 20% in a healthy person [51]. Similarly, if the $RR[n-1]$ is 0.3160.695 s and larger than 0.695 s, then the respective L_w settings are $RR[n-1] \times (1.2)^2$ and $RR[n-1] \times (1.2)$. This L_w optimization (5) contributes to reduction of the computational amount and to improvement of the IHR estimation accuracy.

Unfortunately, the computational cost of the proposed method is about one hundred times as great as that for general threshold methods. Nevertheless, this method can be implemented in the digital domain. We estimate that the power consumption of the proposed method is one-tenth that of the analog portion, which includes an instrumental amplifier, analog filter, and ADC. Furthermore, the power consumption of the analog portion will be reduced using the proposed method because it has higher noise tolerance. Therefore, the total power consumption of the wearable monitor can be reduced.

4. Performance Evaluation

To evaluate the noise tolerance of heart rate extraction algorithms, we implemented the proposed STAC algorithm and conventional algorithms using MATLAB. The objective of the proposed method is IHR extraction every second. Therefore, the proposed method cannot detect all heart beats in the ECG if the interval of R-waves is less than 1 s. To compare the IHR extraction success rate every second, the IHR of the conventional threshold-based method is calculated from the recent interval of R-waves at evaluation time t_n in (7).

4.1 IHR Extraction Success Rate with Clean ECG

First, we investigated the success rate of heart rate extraction using 48 records from the MIT-BIH arrhythmia database [47]. As described above, the proposed STAC can be combined with any other preprocessing filter technique shown in Table 1. The DWT [16] and CWT [22] are implemented as filters in this simulation because the DWT can be realized by simple implementation in hardware and because the CWT is the most noise-tolerant filter technique for ECG.

The threshold of conventional methods is calculated as explained below: In Pan-Tompkins, the threshold is calculated using $(ECG_{max}/8 + (Prev_{TH} - Prev_{TH}/8))$. Here, $Prev_{TH}$ and ECG_{max} respectively denote the previous value of the threshold and the maximum value of ECG in 2 s. In SQRS, the threshold is calculated using $((Prev_{TH} + ECGABS_{max}/4 - Prev_{TH})/8)$. Here, $ECGABS_{max}$ denotes the maximum of the absolute value of ECG in 2 s search range. In WQRS, the average value of ECG in 8 s is used first. Subsequently, the threshold is updated by adding $(ECG_{max} - Prev_{TH}/3)$. In QLV, the ECG is divided into blocks of 0.04 s duration. The threshold is calculated using half of the mean deviation (MD) value of eight blocks that have a larger MD value than the threshold. In DWT, the threshold is calculated using the eighth of the root mean square value of ECG in prior 2 s.

Table 2 IHR extraction success rate of proposed STAC with DWT and CWT filters for MIT-BIH waveforms.

	Success rate [%]			Success rate [%]	
Record	w/ DWT	w/ CWT	Record	w/ DWT	w/ CWT
100	99.44	99.89	202	94.50	96.33
101	99.61	99.67	203	63.00	77.50
102	93.28	94.84	205	97.50	99.56
103	99.94	99.94	207	85.62	89.45
104	93.11	93.56	208	52.97	47.08
105	96.00	97.72	209	99.28	99.78
106	79.66	82.32	210	85.34	90.89
107	94.17	98.72	212	99.89	100.00
108	80.34	81.51	213	93.06	95.45
109	98.22	99.06	214	89.28	92.95
111	95.72	96.50	215	96.78	96.78
112	100.00	100.00	217	89.72	90.44
113	98.72	98.45	219	91.83	94.22
114	93.83	99.06	220	98.28	98.89
115	99.83	99.17	221	84.40	85.84
116	96.45	97.17	222	88.62	88.73
117	94.84	94.28	223	91.50	95.28
118	98.00	98.67	228	82.83	70.56
119	67.96	70.41	230	99.94	100.00
121	99.72	99.94	231	99.17	99.56
122	100.00	100.00	232	71.02	72.65
123	99.61	99.22	233	57.13	88.34
124	97.94	98.67	234	99.78	99.72
200	42.64	88.12	Average	89.72	92.48
201	75.94	82.00			

Table 3 Relation between success rate and type of arrhythmia in 48 records of MIT-BIH.

Type of arrhythmia	# of beats	Success rate [%]			
		Conventional		Proposal	
		DWT	CWT	w/ DWT	w/ CWT
Normal beat	52927	93.18	96.16	97.52	97.88
Left bundle branch block beat	6372	82.42	97.65	96.39	97.65
Right bundle branch block beat	6366	74.55	96.26	94.53	95.62
Atrial premature beat	2588	92.31	93.59	82.65	83.81
Aberrated atrial premature beat	258	58.53	33.72	41.86	38.76
Nodal (junctional) premature beat	64	68.75	95.31	85.94	87.50
Premature ventricular contraction	9847	62.96	63.18	41.85	61.10
Fusion of ventricular and normal beat	715	84.90	92.31	90.49	94.97
Atrial escape beat	21	100.00	90.48	90.48	90.48
Nodal (junctional) escape beat	252	82.94	92.46	83.33	84.52
Ventricular escape beat	108	87.96	92.59	88.89	93.52
Paced beat	5880	71.04	92.45	94.63	96.02
Fusion of paced and normal beat	854	56.91	76.93	85.48	86.30
Unclassifiable beat	35	8.57	57.14	51.43	77.14
Ventricular flutter wave	147	14.29	26.53	42.86	34.69

In CWT, the threshold is calculated using 30% of the maximum value of ECG in the prior 2 s.

Table 2 presents the simulation results. Compared with the conventional algorithms depicted in Fig. 3, no significant difference was found in the success rate obtained with record #100. However, for two reasons, the success rate was degraded for several records (e.g. #119, #208, and #233). The first reason for the performance degradation is a certain type of arrhythmia, which has irregular heart beat waveform (e.g. premature ventricular contraction). As Table 3 shows, although the proposed method shows equivalent or better

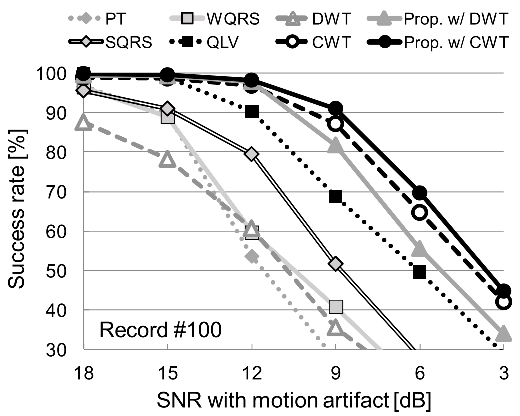

Fig. 9 Noise stress test using MIT-BIH record #100 with motion artifact.

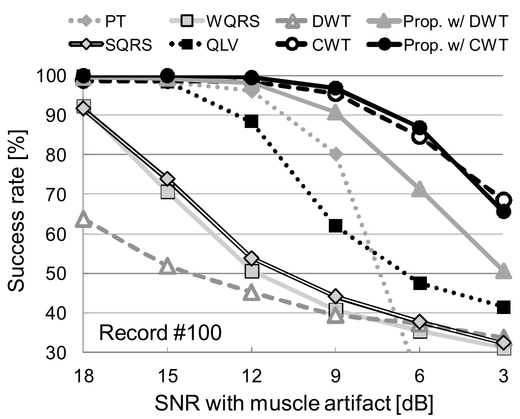

Fig. 10 Noise stress test using MIT-BIH record #100 with muscle artifact.

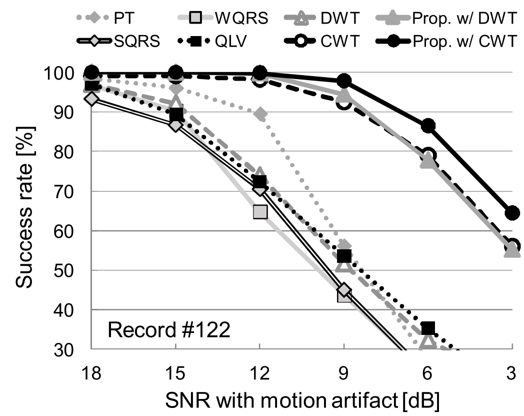

Fig. 11 Noise stress test using MIT-BIH record #122 with motion artifact.

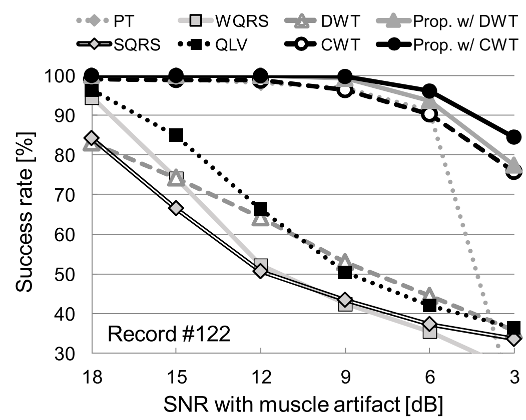

Fig. 12 Noise stress test using MIT-BIH record #122 with muscle artifact.

performance in most cases, it is degraded by such types of arrhythmia because the proposed algorithm uses similarity of the QRS waveform. Therefore, it is difficult to detect a sudden change in the QRS waveform.

The second reason is heart rate variation. Although we assume that the maximum rate of the beat-to-beat variation is 20%, several records include 30% or greater variation. Although this problem can be solvable through parameter tuning, a tradeoff exists between the success rate and the computational amount.

4.2 Performance Comparison in Noise Stress Tests

Next, we evaluated the noise tolerance using the MIT-BIH noise stress test database [52]. Figures 9–12 show the relation between the noise intensity and the success rate of IHR extraction. The MIT-BIH records #100 and #122 are used to evaluate the effects of noise contamination and to eliminate the effects of arrhythmia because these records include few arrhythmia beats. A muscle artifact and motion artifact records are used because these noises have critical frequency characteristics, as presented in Fig. 5. Then, the signal-to-noise ratio (SNR) is defined as shown below.

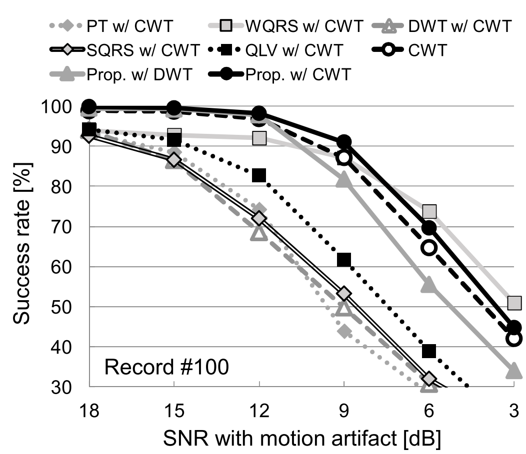

Fig. 13 Noise stress test using MIT-BIH record #100 with motion artifact. Conventional detection methods are combined with CWT filter.

$$SNR = 10 \log \frac{S}{N \times a^2} \tag{8}$$

Here, S, N, and a respectively denote the signal power, frequency-weighted noise power, and scale factor.

Simulation results show that the proposed STAC can improve noise tolerance in both cases of combination: with

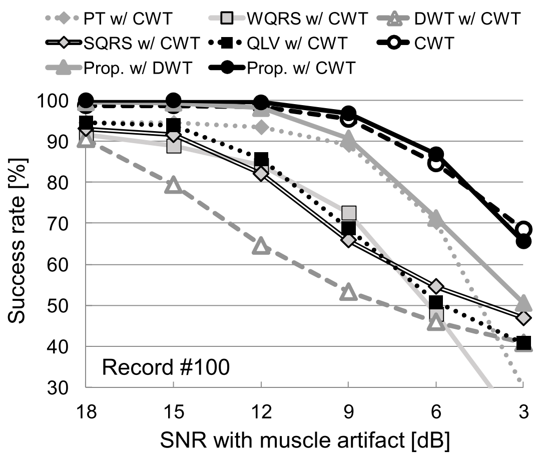

Fig. 14 Noise stress test using MIT-BIH record #100 with muscle artifact. Conventional detection methods are combined with CWT filter.

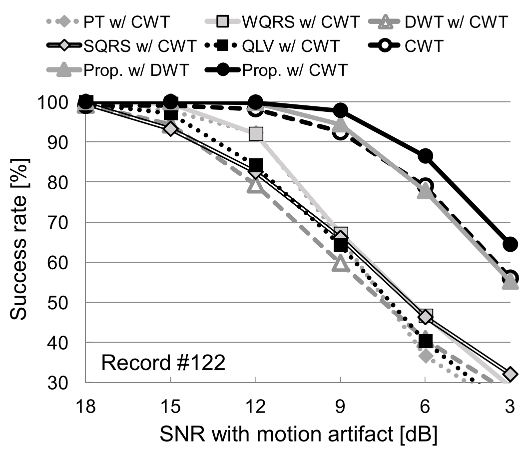

Fig. 15 Noise stress test using MIT-BIH record #122 with motion artifact. Conventional detection methods are combined with CWT filter.

the DWT filter and with the CWT filter. The combination of the STAC and CWT filter achieves the top of noise tolerance with both the muscle artifact and the motion artifact.

Furthermore, in Figs. 13–16, the proposed method is compared to the combination of the CWT filter with conventional QRS detection (threshold) methods, as shown in Table 1. Results show that the success rate of conventional detection methods with CWT filter is improved from original method. This result demonstrates that the CWT filter itself can improve the performance. Note that the combination of the CWT filter and the proposed STAC method still shows better performance in most cases compared with other combinations. Therefore, both the CWT filter and the proposed STAC method contribute synergistically to improved performance.

4.3 Required Resolution of ECG for Hardware Implementation

Finally, we evaluate the required resolution of the ECG signal. The computational amount and the hardware overhead

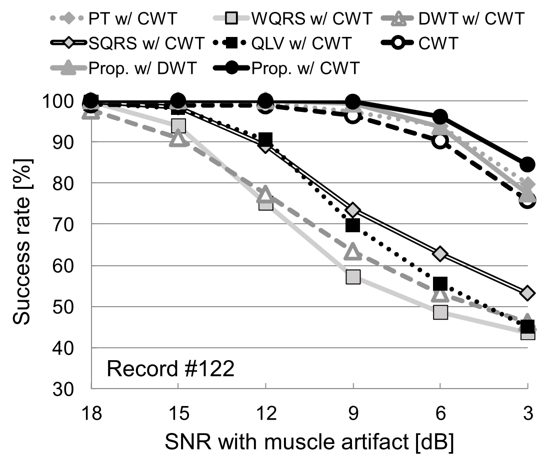

Fig. 16 Noise stress test using MIT-BIH record #122 with muscle artifact. Conventional detection methods are combined with CWT filter.

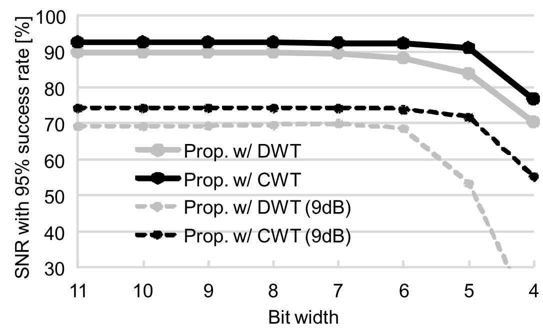

Fig. 17 Bit width of ECG signal versus average success rate of all MIT-BIH waveforms in Table 2 with and without 9-dB motion artifact. The sampling rate is set to 128 samples/s.

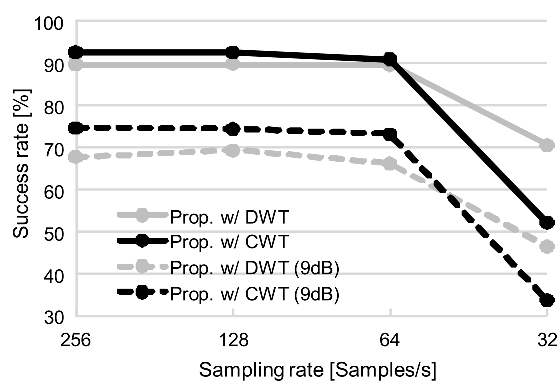

Fig. 18 Sampling rate of ECG signal versus average success rate of all MIT-BIH waveforms in Table 2 with and without 9-dB motion artifact. The bit resolution is set to eight bits.

of IHR extraction should be minimized because the battery capacity is strictly limited in our target application. The bit width and the sampling rate of ECG signal directly affect the overhead.

Figure 17 presents simulation results of the average IHR extraction success rate from 48 records in Table 2 with 4-bit to 11-bit width. The sampling rate of the ECG signal is set to 128 samples/s in this simulation. Results show that the success rate is degraded when the bit width is less than six in both clean and noisy conditions.

Figure 18 portrays the effects of sampling rate differences. The bit width is fixed to eight bits. Other simulation conditions are presented in Fig. 17. Simulation results show that a 128 samples/s sampling rate is needed for extraction of IHR without degradation.

5. Conclusion

As this report has described, we proposed a noise-tolerant IHR extraction algorithm using short-term autocorrelation (STAC). We limited the window length to 1.5 s according to the heart rate of a healthy person, which is 40–240 bpm in general. The window length should be longer than the maximum R2R interval because at least one heart beat should be presented in the window. To realize accurate heart rate extraction using the minimum window length, there are two improved points against the previous autocorrelation algorithm. First, two weight coefficients are introduced to minimize incorrect peak detection both in the window and in the search range. Next, we combined the STAC with DWT and CWT filters because the window length reduction causes noise tolerance degradation. Therefore, we can achieve both noise tolerance improvement and computational reduction. Simulation results show that the IHR extraction success rate of the proposed STAC with the CWT filter is 99.89% for MIT-BIH record #100 and 92.48% on average for 48 records of MIT-BIH. In the noise stress test, the proposed method achieves state-of-the-art noise tolerance both with the muscle artifact and the motion artifact. The required resolution of ECG signal is also evaluated. The proposed method requires seven-bit width and a 128 samples/s sampling rate for ECG signals to extract the IHR without success rate degradation.

Acknowledgments

This research was partially supported by the Ministry of Economy, Trade and Industry (METI) and the New Energy an Industrial Technology Development Organization (NEDO) and a grant from the Tateishi Science and Technology Foundation.

References

[1] H. Nakajima, T. Shiga, and Y. Hata, "Systems health care," Proc. IEEE SMC, pp.1167–1172, Oct. 2011.
[2] W. Roel and M. John, "Comparing spectra of a series of point events particularly for heart rate variability data," IEEE Trans. Biomed. Eng., vol.BME-31, no.4, pp.384–387, April 1984.
[3] S. Yazaki and T. Matsunaga, "Evaluation of activity level of daily life based on heart rate and acceleration," Proc. SICE, pp.1002–1005, Aug. 2010.
[4] K. Itao, T. Umeda, G. Lopez, and M. Kinjo, "Human recorder system development for sensing the autonomic nervous system," Proc. IEEE Sensors, pp.423–426, Oct. 2008.
[5] K. Itao and T. Ito, "Integrated sensing systems for health and safety," Proc. DTIP Symposium, pp.212–216, May 2011.
[6] H. Kim, R.F. Yazicioglu, S. Kim, N.V. Helleputte, A. Artes, M. Konijnenburg, J. Huisken, J. Penders, and C.V. Hoof, "A configurable and low-power mixed signal SoC for portable ECG monitoring applications," IEEE Symp. VLSI Circuits, pp.142–143, June 2011.
[7] S.Y. Hsu, Y.L. Chen, P.Y. Chang, J.Y. Yu, T.F. Yang, R.J. Chen, and C.Y. Lee, "A micropower biomedical signal processor for mobile healthcare applications," Proc. IEEE ASSCC, pp.301–304, Nov. 2011.
[8] M. Ashouei, J. Hulzink, M. Konijnenburg, J. Zhou, F. Duarte, A. Breeschoten, J. Huisken, J. Stuyt, H. de Groot, F. Barat, J. David, and J. van Ginderdeuren, "A voltage-scalable biomedical signal processor running ECG using 13 pJ/cycle at 1 MHz and 0.4V," IEEE ISSCC Dig. Tech. Papers, pp.332–334, Feb. 2011.
[9] M. van Elzakker, E. van Tuijl, P. Geraedts, D. Schinkel, E.A.M. Klumperink, and B. Nauta, "A 1.9 uW 4.4 fJ/conversion-step 10 b 1 MS/s charge-redistribution ADC," IEEE J-SSC, vol.45, no.5, pp.1007–1015, May 2010.
[10] P. Harpe, G. Dolmans, K. Philips, and H. de Groot, "A 7-to-10b 0-to-4 ms/s flexible SAR ADC with 6.5-to-16fJ/conversion-step," IEEE ISSCC Dig. Tech. Papers, pp.472–474, Feb. 2012.
[11] M. Nakano, T. Konishi, S. Izumi, H. Kawaguchi, and M. Yoshimoto, "Instantaneous heart rate detection using short-time autocorrelation for wearable healthcare systems," Proc. IEEE EMBC, pp.6703–6706, Aug. 2012.
[12] J. Pan and W.J. Tompkins, "A real-time QRS detection algorithm," IEEE Trans. Biomed. Eng., vol.BME-32, no.3, pp.230–236, March 1985.
[13] PhysioNet WFDB Applications, sqrs, "http://www.physionet.org/physiotools/wag/sqrs-1.htm" (accessed May 15. 2014)
[14] PhysioNet WFDB Applications, wqrs, "http://www.physionet.org/physiotools/wag/wqrs-1.htm" (accessed May 15. 2014)
[15] C. Li, C. Zheng, and C. Tai, "Detection of ECG characteristic points using wavelet transforms," IEEE Trans. Biomed. Eng., vol.42, no.1, pp.21–28, Jan. 1995.
[16] J.P. Martinez, R. Almeida, S. Olmos, A.P. Rocha, and P. Laguna, "A wavelet-based ECG delineator: Evaluation on standard databases," IEEE Trans. Biomed. Eng., vol.51, no.4, pp.570–581, April 2004.
[17] S.Y. Hsu, Y. Ho, Y. Tseng, T.Y. Lin, P.Y. Chang, J.W. Lee, J.H. Hsiao, S.M. Chuang, T.Z. Yang, P.C. Liu, T.F. Yang, R.J. Chen, C. Su, and C.Y. Lee, "A sub-100μW multi-functional cardiac signal processor for mobile healthcare applications," IEEE Symp. VLSI Circuits, pp.156–157, June 2012.
[18] S.Y. Hsu, Y. Ho, P.Y. Chang, P.Y. Hsu, C.Y. Yu, Y. Tseng, T.Z. Yang, T.F. Yang, R.J. Chen, C. Su, and C.Y. Lee, "A 48.6-to-105.2μW machine-learning assisted cardiac sensor SoC for mobile healthcare monitoring," IEEE Symp. VLSI Circuits, pp.252–253, June 2013.
[19] H. Kim, R.F. Yazicioglu, P. Merken, C.V. Hoof, and H.J. Yoo, "ECG signal compression and classification algorithm with quad level vector for ECG holter system," IEEE Trans. Inf. Technol. Biomed., vol.14, no.1, pp.93–100, Jan. 2010.
[20] H. Kim, R.F. Yazicioglu, T. Torfs, P. Merken, H.J. Yoo, and C.V. Hoof, "A low power ECG signal processor for ambulatory arrhythmia monitoring system," IEEE Symp. VLSI Circuits, pp.19–20, June 2010.
[21] I. Romero, P.S. Addison, M.J. Reed, N. Grubb, G.R. Clegg, C.E. Robertson, and J.N. Watson, "Continuous wavelet transform modulus maxima analysis of the electrocardiogram: Beat characterisation and beat-to-beat measurement," Int. J. Wavelets Multiresolut Inf. Process 3, no.1, pp.19–42, 2005.
[22] I. Romero, B. Grundlehner, and J. Penders, "Robust beat detector for ambulatory cardiac monitoring," Proc. IEEE EMBC, pp.950–953, Sept. 2009.
[23] I. Romero, B. Grundlehner, J. Penders, J. Huisken, and Y.H. Yassin, "Low-power robust beat detection in ambulatory cardiac monitoring," Proc. IEEE BioCAS, pp.249–252, Nov. 2009.
[24] G.B. Moody and R.G. Mark, "Development and evaluation of a

2-lead ECG analysis program," Computers in Cardiology, pp.39–44, 1982.
[25] P.S. Hamilton and W. Tompkins, "Quantitative investigation of QRS detection rules using the MIT/BIH arrhythmia database," IEEE Trans. Biomed. Eng., vol.BME-33, pp.1157–1165, Dec. 1986.
[26] P.E. Trahanias, "An approach to QRS complex detection using mathematical morphology," IEEE Trans. Biomed. Eng., vol.40, pp.201–205, 1993.
[27] R. Poli, S. Cagnoni, and G. Valli, "Genetic design of optimum linear and nonlinear QRS detectors," IEEE Trans. Biomed. Eng., vol.42, pp.1137–1141, Nov. 1995.
[28] J. Lee, K. Jeong, J. Yoon, and M. Lee, "A simple real-time QRS detection algorithm," Proc. IEEE EMBC, pp.1396–1398, 1996.
[29] M. Bahoura, M. Hassani, and M. Hubin, "DSP implementation of wavelet transform for real time ECG wave forms detection and heart rate analysis," Comput. Meth. Programs Biomed., no.52, pp.35–44, 1997.
[30] V.X. Afonso, W.J. Tompkins, T.Q. Nguyen, and S. Luo, "ECG beat detection using filter banks," IEEE Trans. Biomed. Eng., vol.46, pp.192–201, Feb. 1999.
[31] D.S. Benitez, P.A. Gaydecki, A. Zaidi, and A.P. Fitzpatrick, "The use of the Hilbert transform in ECG signal analysis," Comput. Biol. Med., vol.31, pp.399–406, 2001.
[32] D.S. Benitez, P.A. Gaydecki, A. Zaidi, and A.P. Fitzpatrick, "A new QRS detection algorithm based on the Hilbert transform," Computers in Cardiology, vol.27, pp.379–382, 2000.
[33] J. Moraes, M. Freitas, F. Vilani, and E. Costa, "A QRS complex detection algorithm using electrocardiogram leads," Computers in Cardiology, vol.29, pp.205–208, 2002.
[34] P. Hamilton, "Open source ECG analysis," Computers in Cardiology, vol.29, pp.101–104, 2002.
[35] J.C.T.B. Moraes, M.M. Freitas, F.N. Vilani, and E.V. Costa, "A QRS complex detection algorithm using electrocardiogram leads," Computers in Cardiology, pp.205–208, Sept. 2002.
[36] W. Zong, G.B. Moody, and D. Jiang, "A robust open-source algorithm to detect onset and duration of QRS complexes," Computers in Cardiology, pp.737–740, 2003.
[37] B. Hickey, C. Heneghan, and P. de Chazal, "Non-episode-dependent assessment of paroxysmal artial fibrillation through measurement of RR interval dynamics and atrial premature contractions," Ann. Biomed. Eng., vol.32, no.5, pp.677–687, 2004.
[38] M. Paoletti and C. Marchesi, "Discovering dangerous patterns in long-term ambulatory ECG recordings using a fast QRS detection algorithm and explorative data analysis," Computer Methods and Programs in Biomedicine, vol.82, pp.20–30, 2006.
[39] M. Visinescu, C.A. Bashour, M. Bakri, and B.G. Nair, "Automatic detection of QRS complexes in ECG signals collected from patients after cardiac surgery," Proc. IEEE EMBC, pp.3724–3727, Aug. 2006.
[40] N.M. Arzeno, Z.-D. Deng, and C.-S. Poon, "Analysis of first-derivative based QRS detection algorithms," IEEE Trans. Biomed. Eng., vol.55, no.2, pp.478–484, Feb. 2008.
[41] M. Elgendi, S. Mahalingam, M. Jonkman, and F.D. Boer, "A robust QRS complex detection algorithm using dynamic thresholds," Proc. CSA, pp.153–158, Oct. 2008.
[42] M. Adnane, Z. Jiang, and S. Choi, "Development of QRS detection algorithm designed for wearable cardiorespiratory system," Computer Methods and Programs in Biomedicine, vol.93, pp.20–31, 2009.
[43] F. Zhang and L. Yong, "QRS detection based on multiscale mathematical morphology for wearable ECG devices in body area networks," IEEE Trans. Biomed. Circuits Syst., vol.3, pp.220–228, 2009.
[44] J. Lewandowski, H.E. Arochena, R.N.G. Naguib, and K. Chao, "A simple real-time QRS detection algorithm utilizing curve-length concept with combined adaptive threshold for electrocardiogram signal classification," Proc. IEEE TENCON, pp.1–6, Nov. 2012.
[45] M.S. Manikandan and K.P. Soman, "A novel method for detecting R-peaks in electrocardiogram (ECG) signal," Biomedical Signal Processing and Control, vol.7, pp.118–128, 2012.
[46] C. Ieong, P. Mak, C. Lam, C. Dong, M. Vai, P. Mak, S. Pun, F. Wan, and R.P. Martins, "A 0.83-μW QRS detection processor using quadratic spline wavelet transform for wireless ECG acquisition in 0.35-μm CMOS," IEEE Trans. Biomed. Circuits Syst., vol.6, pp.586–595, Dec. 2012.
[47] MIT-BIH Arrhythmia Database (mitdb), "http://www.physionet.org/physiobank/database/mitdb/" (accessed May 15. 2014)
[48] Y. Takeuchi and M. Hogaki, "An adaptive correlation rate meter: a new method for Doppler fetal heart rate measurements," Ultrasonics, pp.127–137, May 1978.
[49] M. Sekine and K. Maeno, "Non-contact heart rate detection using periodic variation in Doppler frequency," Proc. IEEE SAS, pp.318–322, Feb. 2011.
[50] H.L. Chan, G.U. Chen, M.A. Lin, and S.C. Fang, "Heartbeat detection using energy thresholding and template match," Proc. IEEE EMBC, pp.6668–6670, Aug. 2005.
[51] M. Malik, "Heart rate variability; standards of measurement, physiological interpretation, and clinical use," Circulation, vol.93, pp.1043–1065, 1996.
[52] MIT-BIH Noise Stress Test Database (nstdb), "http://www.physionet.org/physiobank/database/nstdb/" (accessed May 15. 2014)

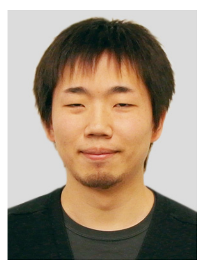

Shintaro Izumi respectively received his B.Eng. and M.Eng. degrees in Computer Science and Systems Engineering from Kobe University, Hyogo, Japan, in 2007 and 2008. He received his Ph.D. degree in Engineering from Kobe University in 2011. He was a JSPS research fellow at Kobe University from 2009 to 2011. Since 2011, he has been an Assistant Professor in the Organization of Advanced Science and Technology at Kobe University. He has served as a Program Committee Member for IEEE Symposium on Low-Power and High-Speed Chips (COOL Chips). His current research interests include biomedical signal processing, communication protocols, low-power VLSI design, and sensor networks.

Masanao Nakano received his B.Eng. degrees in Computer and Systems Engineering from Kobe University, Hyogo, Japan, in 2012. Currently, he is a master course student at Kobe University. His current research is related to wearable health-care systems. ng, communication protocols, low-power VLSI design, and sensor networks.

Ken Yamashita received his B.Eng. degree in Informatics from Sizuoka University, Sizuoka, Japan, in 2012. Currently, he is a master course student at Kobe University. His current research is related to wearable health-care systems.

Yozaburo Nakai received his B.Eng. degree in Computer and Systems Engineering from Kobe University, Hyogo, Japan, in 2014. Currently, he is a master course student at Kobe University. His current research is related to wearable health-care systems and biosignal processing.

Hiroshi Kawaguchi received B.Eng. and M.Eng. degrees in electronic engineering from Chiba University, Chiba, Japan, in 1991 and 1993, respectively, and earned a Ph.D. degree in Engineering from The University of Tokyo, Tokyo, Japan, in 2006. He joined Konami Corporation, Kobe, Japan, in 1993, where he developed arcade entertainment systems. He moved to The Institute of Industrial Science, The University of Tokyo, as a Technical Associate in 1996, and was appointed as a Research Associate in 2003. In 2005, he moved to Kobe University, Kobe, Japan. Since 2007, he has been an Associate Professor with The Department of Information Science at that university. He is also a Collaborative Researcher with The Institute of Industrial Science, The University of Tokyo. His current research interests include low-voltage SRAM, RF circuits, and ubiquitous sensor networks. Dr. Kawaguchi was a recipient of the IEEE ISSCC 2004 Takuo Sugano Outstanding Paper Award and the IEEE Kansai Section 2006 Gold Award. He has served as a Program Committee Member for IEEE Custom Integrated Circuits Conference (CICC) and IEEE Symposium on Low-Power and High-Speed Chips (COOL Chips), and as a Guest Associate Editor of IEICE Transactions on Fundamentals of Electronics, Communications and Computer Sciences and IPSJ Transactions on System LSI Design Methodology (TSLDM).

Masahiko Yoshimoto joined the LSI Laboratory, Mitsubishi Electric Corporation, Itami, Japan, in 1977. From 1978 to 1983 he had been engaged in the design of NMOS and CMOS static RAM. Since 1984 he had been involved in the research and development of multimedia ULSI systems. He earned a Ph.D. degree in Electrical Engineering from Nagoya University, Nagoya, Japan in 1998. Since 2000, he had been a professor of Dept. of Electrical & Electronic System Engineering in Kanazawa University, Japan. Since 2004, he has been a professor of Dept. of Computer and Systems Engineering in Kobe University, Japan. His current activity is focused on the research and development of an ultra low power multimedia and ubiquitous media VLSI systems and a dependable SRAM circuit. He holds on 70 registered patents. He has served on the program committee of the IEEE International Solid State Circuit Conference from 1991 to 1993. Also he served as Guest Editor for special issues on Low-Power System LSI, IP and Related Technologies of IEICE Transactions in 2004. He was a chair of IEEE SSCS (Solid State Circuits Society) Kansai Chapter from 2009 to 2010. He is also a chair of The IEICE Electronics Society Technical Committee on Integrated Circuits and Devices from 2011-2012. He received the R&D100 awards from the R&D magazine for the development of the DISP and the development of the realtime MPEG2 video encoder chipset in 1990 and 1996, respectively. He also received 21th TELECOM System Technology Award in 2006.